Pis'ma v ZhETF, vol. 102, iss. 7, pp. 463 – 466

Scattering phase shifts in the complex scaling method

M. Odsuren[+1)], *K. Katō*[*], *G. Khuukhenkhuu*[+]

[+]*School of Engineering and Applied Sciences, Nuclear Research Center, National University of Mongolia, 210646 Ulaanbaatar, Mongolia*

[*]*Nuclear Reaction Data Centre, Faculty of Science, Hokkaido University, 060-0810 Sapporo, Japan*

Submitted 27 July 2015

We investigate the scattering phase shifts by using the complex scaling method. The real-range and complex-range Gaussian basis functions are utilized for the investigation of the low-lying excited states of ^{5}He.

DOI: 10.7868/S0370274X15190017

Introduction. In the last half-century, study of resonances in the scattering problem of light nuclei has been carried out using various methods, one of which is the complex scaling method (CSM) [1–4]. The theory of the complex scaling was proposed mathematically [2] and it has been extensively applied to the atomic and nuclear physics [4–6]. The CSM is one of the well-established techniques in wide areas of physics, especially in resonance studies in nuclear physics. At the beginning, its advantage was mainly explained by the superior description of the resonances of the composite systems. Nowadays, it is successfully utilized for getting information on the unbound and scattering states in the observables.

In the present framework, the complex scaled orthogonality condition model (CSOCM) [7] and the extended completeness relation [8] are used. The scattering phase shifts have been investigated as important scattering quantities from the continuum level density (CLD) [9] obtained using the CSM. The CSOCM can be used for obtaining scattering phase shifts of the many resonance system [6].

In this work, we study the $\alpha + n$ interactions using the CSM by analyzing observed scattering phase shifts not only for low-partial waves but also for higher-partial waves. We analyze a realistic system by using two kinds of basis functions. The $\alpha + n$ potential well explains observed data of low energy $\alpha + n$ scattering. However, it does not well reproduce observed phase shifts for higher-partial waves as for low-partial waves.

Two-body formalism. *Complex scaling method.* The CSM has been proposed to solve for the resonance states and to discuss their structures [4, 5]. The relative coordinate $\mathbf{r}_i$ is transformed as $\mathbf{r} \to \mathbf{r}e^{i\theta}$ with a real parameter θ. The $U(\theta)$ operates on a function ψ, that is,

$$\psi(\theta) = U(\theta)\psi(r) = e^{\frac{3}{2}i\theta}\psi(re^{i\theta}). \quad (1)$$

The complex scaled Hamiltonian of inter cluster motion is given by

$$\hat{H}(\theta) = U(\theta)\hat{H}U^{-1}(\theta). \quad (2)$$

The complex-scaled Schrödinger equation is expressed using the complex-scaled Hamiltonian $\hat{H}^\theta$ as

$$\hat{H}^\theta\psi(\theta) = E\psi(\theta). \quad (3)$$

The resonant states are obtained as the eigenvalues and eigenstates by solving the complex scaled Schrödinger equation (3). The complex energies of resonant states are obtained as $E = E_r - i\Gamma/2$ when $\tan^{-1}(\Gamma/2E_r) < 2\theta$. Therefore, employing an appropriate scaling parameter θ, we can derive resonant states in terms of Gaussian functions

$$\psi(\theta) = \sum_{i=1}^{N} c_i(\theta)\phi_i. \quad (4)$$

In Fig. 1, we present a schematic eigenvalue distribution for the complex scaled Schrödinger equation. It is seen that the energies of bound states are not changed from the spectral positions of the original Hamiltonian. The continuum spectra of the Hamiltonian $\hat{H}^\theta$ are distributed on the 2θ-lines originating from every threshold. If we do not apply the complex scaling, the original Schrödinger equation gives the continuum spectra, including resonances on the positive energy axis. Under complex scaling, the resonances are separated from the continuum, and the rotated continuum spectra starting from different threshold energies are separately obtained on different 2θ-lines. Furthermore, when we apply basis function method to solve the complex scaled

[1)]e-mail: odsurenn@gmail.com

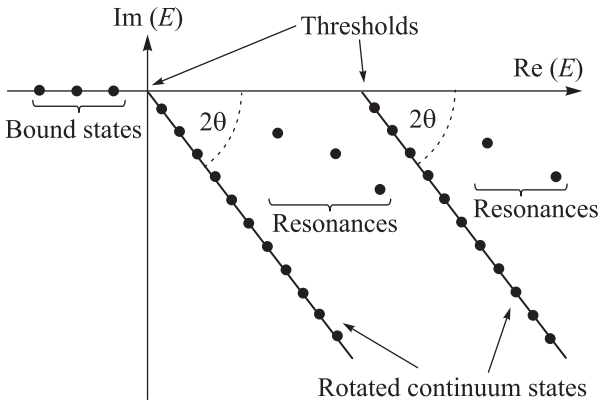

Fig. 1. Schematic energy eigenvalue distribution for a complex scaled Hamiltonian

Schrödinger equation, these continuum spectrum are discretized on different 2θ-lines, as shown in Fig. 1.

Continuum level density and scattering phase shift. The continuum level density (CLD) $\Delta(E)$ as function of the real energy E is defined as [9]

$$\Delta(E) = -\frac{1}{\pi}\mathrm{Im}\left\{\mathrm{Tr}[G^+(E) - G_0^+(E)]\right\}, \qquad (5)$$

where

$$G^+(E) = (E + i\varepsilon - H)^{-1}, \quad G_0^+(E) = (E + i\varepsilon - H_0)^{-1}$$

are the full and free Green's functions, respectively. The CLD is also related to the scattering phase shift $\delta(E)$ and the relation is expressed in a single channel case as [9]

$$\Delta(E) = \frac{1}{\pi}\frac{d\delta(E)}{dE}. \qquad (6)$$

Using Eqs. (5) and (6), we can obtain the phase shift $\delta(E)$ in terms of the eigenvalues of H and H_0 by integrating the CLD over the energy E. When we apply the complex scaling and obtain the complex scaled Green's function the CLD can be expressed as

$$\Delta(E) = -\frac{1}{\pi}\mathrm{Im}\left\{\mathrm{Tr}\left(\frac{1}{E - H^\theta} - \frac{1}{E - H_0^\theta}\right)\right\}. \qquad (7)$$

Numerical results. One of the methods to prove the nuclear structure is to use the scattering phenomena. In this part, we are concerned the scattering with the relative motion of two-particles. The α+n scattering phase shift provides a convenient test of several important properties of low-energy nuclear scattering. There are no bound states in the $A = 5$ system, but the $3/2^-$ partial wave has a sharp low-energy resonance in the $\alpha + n$ system.

The resonance states of $3/2^-$ and $1/2^-$ in ^{5}He are calculated by using real- and complex-range Gaussian basis functions. The real-range Gaussian basis functions have been successfully utilized for three, four, five body problems [10–12]. Furthermore, the complex-range Gaussian basis functions have been introduced by Ref. [13] and it is applied in the few body system [14]. The real-range Gaussian basis functions are feasible for describing short-range correlation, but it is difficult to calculate the high oscillator functions with several nodes in accurate accuracy. In order to better understand advantage of complex-range Gaussian basis functions, Ref. [14] was represented test calculation of energy eigenvalues in the harmonic oscillator potential by using the complex-range and real-range Gaussian basis functions, and was shown the complex-range Gaussian basis functions can reproduce more accurately results up to higher excited states than the real-range Gaussian basis functions. The $\alpha + n$ system has been investigated in detail within a microscopic model by Kanada et al. [15]. They have performed the microscopic calculation based on the effective nuclear potentials. In this calculation, we choose the KKNN (Kanada, Kaneko, Nagata, and Nomoto) [15] potential as the central part of the effective nucleon-nucleon interaction. The estimated results in this calculation are shown in Table 1 with experimental data taken from a review paper [16].

Table 1. The experimental and calculated resonance energies and widths for low-lying $3/2^-$ and $1/2^-$ states of ^{5}He

	Experiment [16] [MeV]		This work [MeV]			
			Real-range		Complex-range	
	E_r	Γ_r	E_r	Γ_r	E_r	Γ_r
$3/2^-$	0.798	0.648	0.74	0.59	0.78	0.60
$1/2^-$	1.27	5.57	2.10	5.82	2.05	5.60

The calculated scattering phase shifts for the $3/2^-$ and $1/2^-$ two low-lying states of α+n system are shown in the Fig. 2. We can see from Fig. 2 the microscopic effective KKNN potential well reproduces scattering phenomena in the low-lying states of this system. We compared our results with the experimental data [17] of phase shifts and observed good agreement between them in the each partial state.

In Fig. 3, we show the computed results of the scattering phase shifts of low-lying $3/2^-$ and $1/2^-$ partial waves in the α+n system, which are calculated by using real- and complex-range Gaussian basis functions. The different basis functions are applied to calculations of the eigenvalue problems for the complex scaled Hamiltonians. The same structure appears in the both partial waves where the dashed-lines represent real-range and solid-curves display complex-range Gaussian basis functions are used results, respectively. The computed res-

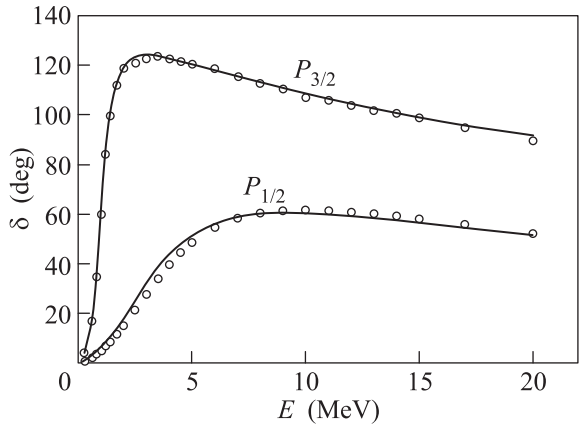

Fig. 2. Scattering phase shifts of ^{5}He at the $J^\pi = 3/2^-$ and $1/2^-$ waves for $\theta = 20^\circ$. The experimental data [17] are shown with open circles

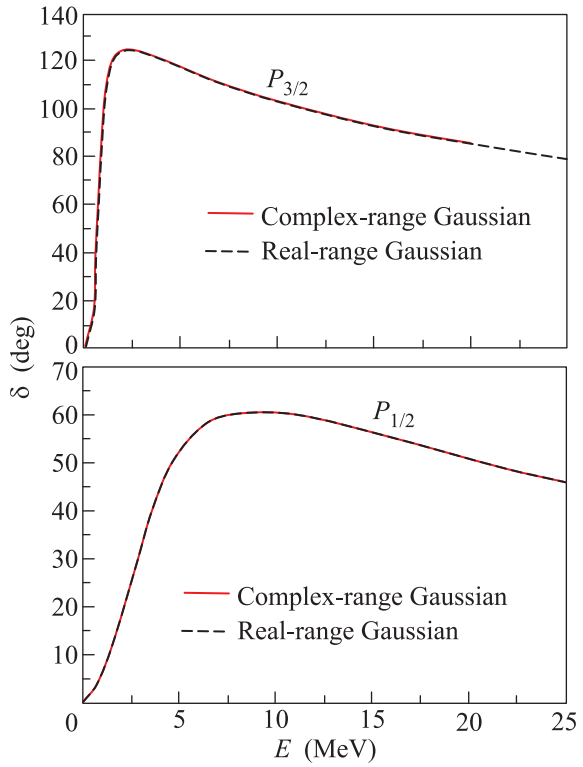

Fig. 3. Scattering phase shifts by real-range (dashed line) and complex-range (read curve) Gaussian basis functions for $\theta = 20^\circ$

onance energies and widths by complex- and real-range Gaussian basis functions are in a good agreement with each other.

Fig. 4 shows the calculated results (solid curves) and experimental data (open circles). We interpreted in Fig. 4, our computed results of p-wave could be explain equally well to the experimental data in which the CSM is used with KKNN potential. However, the

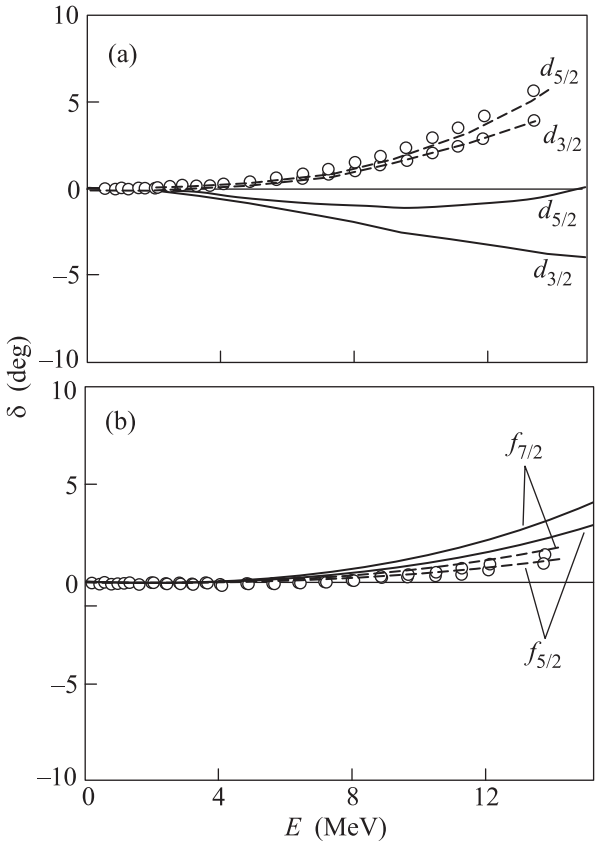

Fig. 4. The scattering phase shifts of the d- and f-waves are calculated not only by ordinal KKNN potential for $\theta = 20^\circ$. Open circles are represent the experimental data [17] and solid curves are calculated results with ordinal KKNN potential, dashed-lines are computed results by improved potential [18]

calculated results of higher partial waves (solid curves) indicate that the theoretical results lower in the d-wave (see Fig. 4a) and higher in the f-wave (see Fig. 4b) than experimental data. The higher partial waves of phase shifts of the $\alpha + n$ have been discussed [17] by experimental cross section and polarization applying R-matrix analysis. As can be seen in Fig. 4a, the computed results give repulsive behavior, but [17] show attractive behavior. In case of the f-wave, calculated results and experimental data both represent positive behavior. In order to explain the discrepancy of the experimental data and calculated results of high partial levels, an improvement of the effective potential was performed [18]. We used the improved effective potential at high states of partial waves of the ^{5}He and results shown in the Fig. 4 by dashed-lines. As can be seen in Fig. 4, the improved effective potential can be applied to describe scattering phase shifts for higher partial levels of this system.

Discussion and summary. We have presented that CSM is a useful method for obtaining the resonant states and the scattering quantities such as the phase shifts. The phase shift of the two-body $\alpha + n$ system has been investigated in the present method. Furthermore, we have investigated the scattering phase shift of $\alpha+n$ system with real- and complex-range Gaussian basis functions. Two different basis functions showed that the resonance behaviors of scattering phase shifts are similar to each other.

The original $\alpha+n$ interaction constructed by Kanada et al. [15] well reproduces p-wave phase shifts, but it does not give good reproduction of observed higher-partial wave phase shifts of d- and f-waves. However, as discussed in the previous section, we have used $\alpha+n$ improved effective potential and it well reproduces the observed d- and f-waves phase shifts.

Authors acknowledge support by National University of Mongolia and Mongolian Foundation for Science and Technology. The numerical calculation was supported by the cluster computing system at the Nuclear Research Center, National University of Mongolia.

1. Y. K. Ho, Phys. Rep. **99**, 1 (1983).
2. J. Aguilar and J. M. Combes, Comm. Math. Phys. **22**, 269 (1971); E. Balslev and J. M. Combes, Comm. Math. Phys. **22**, 280 (1971).
3. N. Moiseyev, Phys. Rep. **302**, 212 (1998).
4. T. Myo, Y. Kikuchi, H. Masui, and K. Katō, Prog. Part. Nucl. Phys. **79**, 1 (2014).
5. S. Aoyama, T. Myo, K. Katō, and K. Ikeda, Prog. Theor. Phys. **116**, 1(2006).
6. M. Odsuren, K. Katō, M. Aikawa, and T. Myo, Phys. Rev. C **89**, 034322 (2014).
7. A. T. Kruppa and K. Katō, Prog. Theor. Phys. **84**, 1145 (1990).
8. T. Myo, A. Ohnishi, and K. Katō, Prog. Theor. Phys. **99**, 801 (1998).
9. R. Suzuki, T. Myo, and K. Katō, Prog. Theor. Phys. **113**, 1273 (2005).
10. Y. Kikuchi, T. Myo, K. Katō, and K. Ikeda, Phys. Rev. C **87**, 034606 (2013).
11. T. Myo, Y. Kikuchi, and K. Katō, Phys. Rev. C **84**, 064306 (2011).
12. T. Myo, Y. Kikuchi, and K. Katō, Phys. Rev. C **85**, 034338 (2012).
13. E. Hiyama, Y. Kino, and M. Kamimura, Prog. Part. Nucl. Phys. **51**, 223 (2003).
14. E. Hiyama, Prog. Theor. Exp. Phys. A **204**, 223 (2012).
15. H. Kanada, T. Kaneko, S. Nagata, and M. Nomoto, Prog. Theor. Phys. **61**, 1327 (1979).
16. D. R. Tilley et al., Nucl. Phys. A **708**, 3 (2002).
17. B. Hoop, Jr. and H. H. Barschall, Nucl. Phys. **83**, 65 (1966); Th. Stammbach and R. L. Walter, Nucl. Phys. A **180**, 225 (1972).
18. S. Aoyama, S. Mukai, K. Katō, and K. Ikeda, Prog. Theor. Phys. **93**, 99 (1995).